Plastics and Rubber Processing and Applications 6 (1986) 101–108

Effect of dynamic crosslinking on ethylene vinyl acetate thermoplastic elastomer

Sabu Thomas, Baby Kuriakose, B. R. Gupta and S. K. De
Rubber Technology Centre, Indian Institute of Technology, Kharagpur 721 302, India

(Received 25 September 1985; accepted 11 October 1985)

Abstract: The effect of dynamic crosslinking on rheological behaviour and technical properties of ethylene vinyl acetate (EVA) thermoplastic elastomer has been evaluated with special reference to the dosage of the crosslinking agent. It is observed that dynamic crosslinking mildly increases the viscosity of the system at high shear rates but gives better physical and processing properties. Empirical correlations have been developed for the viscosity of the elastomer as a function of crosslinking agent concentration. In order to understand the effect of dynamic crosslinking on fracture mechanism, tensile and tear failure surfaces have been examined by a scanning electron microscope (SEM).

Nomenclature

A_P	Cross-sectional area of the plunger (mm^2)
A_0	Weight of the absorbed solvent, corrected for the swelling increment
D	Weight after drying out
DCP	Dicumyl peroxide
d_c	Diameter of capillary (mm)
d_e	Diameter of extrudate (mm)
EVA	Ethylene vinyl acetate
F	Extrusion force (N)
f	Fraction of insoluble components
K	Consistency index
l_c	Length of capillary (mm)
$n' = n$	Flow behaviour index defined $d(\log \tau_w)/d(\log \gamma_{wa})$
P	Dosage in phr of the crosslinking agent
phr	Parts per hundred 'rubber' (EVA)
Q	Volume flow rate (mm^3/s)
T	Weight of the sample
V_r	Volume fraction of EVA in the solvent swollen sample
γ_w	Shear rate at wall (s^{-1})
$\gamma_{wa} = \dfrac{32Q}{\pi d_c^3}$	Apparent shear rate at wall (s^{-1})
η	Shear viscosity (Ns/m^2)
ρ_r	Density of EVA = 0.975 (g/cc)
ρ_s	Density of solvent = 0.866 (g/cc)
τ_w	Apparent shear stress at wall (Pa)

1 Introduction

Thermoplastic elastomers combine the processing advantages of thermoplastics and the physical properties of vulcanized rubbers. These materials may be block copolymers consisting of a hard thermoplastic segment and a soft rubbery segment, or blends of a crystalline polyolefin and an elastomer, or may be those polymers which have specified stereo-regular structure and controlled extent of crystallinity.[1–3] One of the important advantages of thermoplastic elastomers is that they can be processed like thermoplastic materials at temperatures above the crystalline melting point or glass transition temperature of the thermoplastic component of the system, by extrusion or injection moulding techniques. Ethylene vinyl acetate (EVA) copolymers are thermoplastic elastomers which have been commercially available for many years. The thermoplastic elastomeric character of EVA is due to the presence of crystalline polyethylene segments in the polymer chain.[4] These materials are noted for their properties such as high impact strength, better environmental stress crack resistance and good ageing resistance. Their properties can be varied over a wide range by controlling the co-monomer ratio, molecular weight and other structural features which make them useful in many applications.[5] Hence these materials are currently used for making a variety of products such as cables, films, tubings, rail pads, footware, foams and adhesives. It has been reported that EVA copolymers can be crosslinked by conventional methods using peroxides to improve properties such as tensile strength, modulus, tear strength, abrasion resistance and hardness.[5] It has also been shown that addition of very small quantities of crosslinking agent during the mixing operation improves the final properties of thermoplastic

Plastics and Rubber Processing and Applications 0144-6045/86/$03.50

elastomers based on rubber–plastic blends, without adversely affecting the processing characteristics.[6–11] This process is known as dynamic crosslinking. The present work indicates that dynamic crosslinking can be applied to EVA as well, because of the presence of crystalline polyethylene segments in the system. The physical properties and rheological behaviour of polymer blends and those of polymers containing gel and crosslinked particles have been studied by different research groups.[12–16] Various factors affecting the die swell, melt fracture and extrudate deformation have also been reported.[17–21] Recently, Kuriakose and De have studied the effect of dynamic crosslinking based on sulphur, peroxide and mixed systems on the physical properties and melt flow characteristics of natural rubber-polypropylene thermoplastic elastomers.[22–24]

In this paper, we report on the effects of the extent of dynamic crosslinking on the rheological properties such as melt viscosity, flow behaviour index and extrudate swell of ethylene vinyl acetate thermoplastic elastomer. Empirical equations relating the concentration of the crosslinking agent and the melt viscosity have been derived. The effects of the extent of dynamic crosslinking on the tensile and tear properties of EVA have also been studied. The tensile and tear failure processes have been studied by scanning electron microscope (SEM) observations of the failure surfaces.

2 Experimental

2.1 Preparation of the test samples

The details of the EVA copolymer and the crosslinking agent, dicumyl peroxide (DCP), used in the present study are given in Table 1. Pellets of EVA were melted in a Brabender Plasti-corder model PLE 330, for 7 min using a cam-type mixer with a rotor speed of 80 rpm and the chamber temperature set at 180°C. The crosslinking agent was added at the fourth minute of the mixing cycle. Five different mixes containing varying proportions of crosslinking agent were prepared for studies. These are designated as EV_0, EV_1, EV_2, EV_3 and EV_4 and contain 0, 0·125, 0·250, 0·375 and 0·50 phr of DCP, respectively (Table 1). Typical plastographs obtained for the mixes are shown in Fig. 1. After mixing, the molten material was sheeted out through a laboratory mill at nip setting of 2·5 mm. In each case, specimens were cut from the sheeted-out stock for rheological studies. The remaining sheets were compression moulded at 200°C for 3 min in a specially designed mould, so that the mould with the specimen inside could be cooled immediately after moulding, keeping the specimen still under compression. Specimens of size 15 × 15 × 0·2 cm for tensile and tear tests were punched from the moulded sheets.

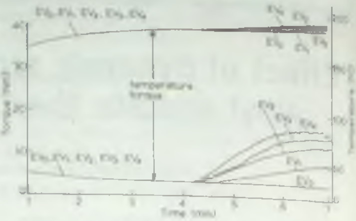

Fig. 1 Typical plastographs obtained for the mixes.

2.2 Rheological studies

Rheological measurements were carried out using a capillary rheometer MCR 3210 attached to an Instron Universal Testing Machine, model 1195. A capillary of length to diameter ratio (l_c/d_c) 40, with an angle of entry of 90°, was used for this study so as to minimise the capillary end effects. The temperature was controlled within ±0·5°C during the melt flow measurements. The specimen for testing was put inside the barrel of the extrusion assembly and forced down to the capillary with a plunger attached to the moving crosshead.

Table 1. Formulation of the mixes

Components	EV_0	EV_1	EV_2	EV_3	EV_4
Ethylene vinyl acetate copolymer[a]	100	100	100	100	100
Dicumyl peroxide[b]	0	0·125	0·25	0·375	0·50

[a] Copolymers of ethylene and vinyl acetate. The vinyl acetate content of the polymer was 45% and the Mooney viscosity ML – 4′ (100°C) was 30. The material was manufactured by Bayer, AG, Federal Republic of Germany.
[b] 40% Active peroxide crosslinking agent. The material was supplied by Bengal Waterproof, Calcutta, India.

After a warming-up period of 5 min, the melt was extruded through the capillary at pre-selected speeds of the crosshead which varied from 0·5 to 500 mm per min. The force corresponding to different plunger speeds was recorded using a strip chart recorder assembly. The force and crosshead speeds were converted into apparent shear stress (τ_w) and shear rate at the wall (γ_w) respectively, using the following equations involving the geometry of the capillary and plunger.[25]

$$\tau_w = \frac{F}{4A_p(l_c/d_c)} \tag{1}$$

$$\gamma_w = \left(\frac{3n'+1}{4n'}\right) \times \frac{32Q}{\pi d_c^3} \tag{2}$$

The flow behaviour index n' was determined by regression analysis of the values of τ_w and γ_w obtained from the experimental data. The shear viscosity, η, was calculated from τ_w and γ_w.

2.3 Swell measurements

The extrudate emerging from the capillary was collected taking maximum care to avoid any further deformation. The diameter of the extrudate was measured at several points using a travelling microscope. The measurements were also made at several intervals of time and it was noticed that there was no change in the diameter after 24 h. The values after 24 h were recorded as equilibrium extrudate diameter, d_e. The swelling index was calculated as the ratio of the diameter of the extrudate to that of the capillary (d_e/d_c).

2.4 Physical testing

Tensile testing of the samples was done at 25°C following the ASTM D 412-80 test method, using dumb bell-shaped test specimens at a crosshead speed of 500 mm per min with an Instron Universal Testing Machine (model 1195). The tear strengths of the specimens were determined following the ASTM D 624-81 test method using un-nicked 90° angle test pieces. The tear test was carried out at the same conditions of temperature and crosshead speed as described for the tensile test.

2.5 Determination of V_r

To establish the extent of crosslinking, the volume fraction, V_r, of EVA in the specimen swollen in toluene was determined after 48 h at 35° ±1°C, using the relation[26]

$$V_r = \frac{(D-fT)\rho_r^{-1}}{(D-fT)\rho_r^{-1} + A_0\rho_s^{-1}} \tag{3}$$

2.6 Scanning electron microscope (SEM) studies

The SEM observations of the failure surfaces of EV_0 and EV_4 were made using a Philips model 500 scanning electron microscope. The failure surfaces of the test specimens were carefully cut from the test pieces and then sputter coated with gold within 24 h of testing. The gold coated surfaces were examined through the scanning electron microscope, adjusting the tilt to zero in all cases. Figure 2 shows the details of the test specimen, failure surface and the area of the tensile and tear specimens which were scanned.

3 Results and discussion

The V_r values of the crosslinked mixes are given in Table 2. The V_r values decrease in the order $EV_4 > EV_3 > EV_2 > EV_1$. This indicates that extent of crosslinking increases with the increasing dosage of the crosslinking agent. The V_r values for both the mixed and the moulded samples are found to be the same, indicating that the process of crosslinking is completed during the mixing operation and no further crosslinking takes place during the moulding. The torque readings obtained for the mixes (Fig. 1) also indicate that the extent of crosslinking increases with the increasing dosage of DCP. The torque attains a steady value after 7 min showing that crosslinking is complete.

3.1 Rheological properties

3.1.1 Effect of shear rate and dynamic crosslinking on viscosity. The effect of shear rate

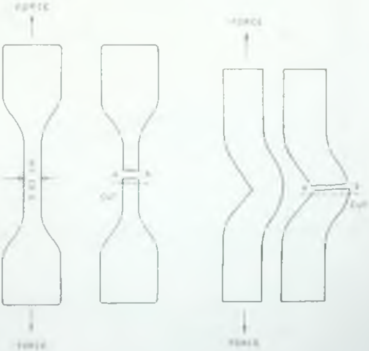

Fig. 2 Specimens for tensile and tear tests showing fracture surfaces and area scanned.

on the viscosity of mixes containing different amounts of crosslinking agent at 200°C is shown in Fig. 3. It is seen that the viscosity of the mixes increases with increasing concentration of crosslinking agent over the entire range of shear rate. The increase in viscosity is more pronounced in the lower shear region than at higher shears. The curve for EV_0 also indicates that the uncrosslinked ethylene vinyl acetate is relatively less shear sensitive, compared with the dynamically crosslinked samples. Figure 4 shows the effect of dosage of DCP on the viscosity of EVA at different shear rates. It is observed that the viscosity increases at a faster rate with lower contents of DCP and at lower shear rates. However, the curves appear to flatten out beyond 0·25 phr of DCP at all shear rates.

3.1.2 Effect of temperature and dynamic crosslinking on flow behaviour index (n′). The effect of temperature and extent of dynamic crosslinking on the n' values are presented by the histograms in Fig. 5. In the case of uncrosslinked EVA (EV_0), the n' value increases marginally with temperature from 170° to 190°C, but shows a sharp rise at 200°C. This indicates the tendency of the material to approach Newtonian behaviour at high temperatures. In the case of dynamically crosslinked samples, the lower values of n' compared with EV_0 indicate higher pseudo-plastic behaviour. Moreover the n' values of the crosslinked samples remain nearly constant with the increasing temperature. This shows that dynamic crosslinking stabilises the rheological behaviour of EVA at higher processing temperatures.

3.1.3 Effect of shear rate and dynamic crosslinking on die swell. Figure 6 shows the swelling index of the mixes at three different shear rates. In all cases, the swelling index increases with increase in shear rate. The effect of dynamic crosslinking on swelling index shows an interesting behaviour. The swelling index initially increases

Table 2 **V_r values of the crosslinked mixes**

Mix number	V_r after mixing	V_r after moulding
EV_1	0·012	0·012
EV_2	0·019	0·018
EV_3	0·027	0·027
EV_4	0·030	0·031

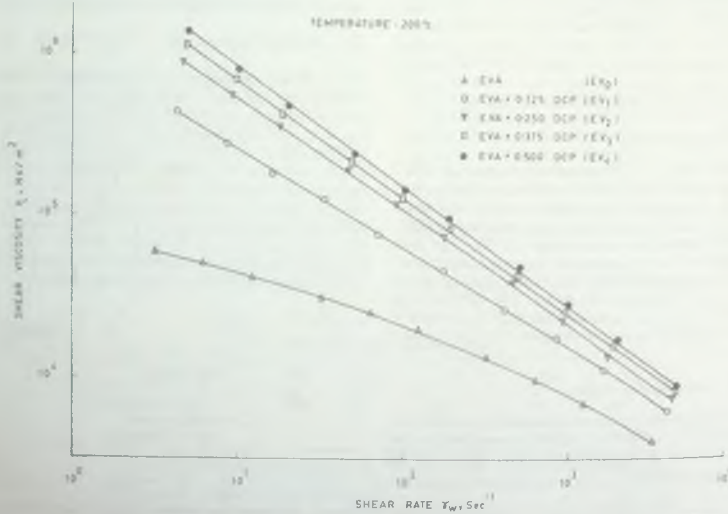

Fig. 3 Viscosity–shear rate plots showing the effect of extent of dynamic crosslinking on viscosity at 200°C.

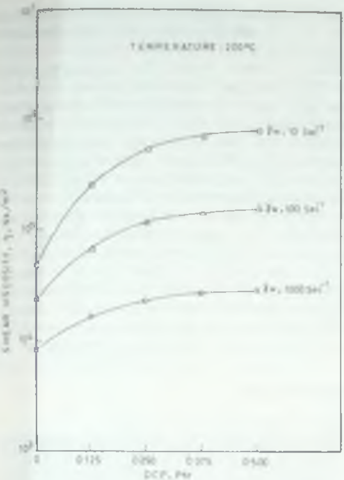

Fig. 4 Effect of DCP dosage on viscosity at 200°C.

with DCP concentration up to 0·125 phr and then decreases. As this behaviour is slightly abnormal, the swelling index was measured several times to establish the reproducibility.

3.1.4 Correlation between shear viscosity and dosage of crosslinking agent. From the experimental results on rheological studies with varying extent of crosslinking, empirical correlations have been derived for the apparent viscosity of the crosslinked system as a function of DCP dosage (P) and apparent wall shear rate ($\dot{\gamma}_{wa}$) at four different temperatures: 170°, 180°, 190° and 200°C. In general, the viscosity equation is expressed as follows:

$$\eta = K\left(\frac{3n'+1}{4n'}\right)(\dot{\gamma}_{wa})^{n'-1} \tag{4}$$

For each temperature under study, the equations for K and n' (Table 3) are determined in terms of the dosage of the crosslinking agent (P) by statistical methods. On substituting these equations in the general viscosity equation (4), the viscosity of dynamically crosslinked material can be found for the desired shear rate and extent of crosslinking (0·125 to 0·5 phr of DCP) according to the processing needs. The calculated values of viscosities from the

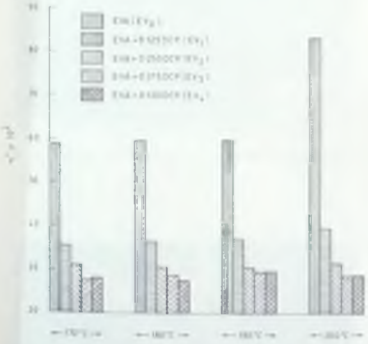

Fig. 5 Effect of temperature and extent of dynamic crosslinking on the melt flow index (n').

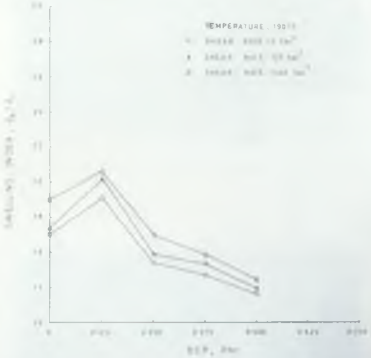

Fig. 6 Effect of shear rate and extent of dynamic crosslinking on the swelling index.

Table 3. Equations for K and n' at different temperatures (valid for $0{\cdot}125 \leqslant P \leqslant 0{\cdot}5$)

At 170°C	$K = 12{\cdot}06 \times 10^6 \times P^{0{\cdot}834}$	$n' = 0{\cdot}239 \times P^{-0{\cdot}186}$
At 180°C	$K = 11{\cdot}815 \times 10^6 \times P^{0{\cdot}899}$	$n' = 0{\cdot}235 \times P^{-0{\cdot}208}$ [illegible]
At 190°C	$K = 9{\cdot}10 \times 10^6 \times P^{0{\cdot}783}$	$n' = 0{\cdot}252 \times P^{-0{\cdot}198}$ [illegible]
At 200°C	$K = 10{\cdot}28 \times 10^6 \times P^{0{\cdot}977}$	$n' = 0{\cdot}234 \times P^{-0{\cdot}238}$

above equations have been verified with the experimental results and the deviation was found to be within 15%.

3.2 Mechanical properties

Table 4 gives the mechanical properties of the mixes. The modulus and tear strength follow the order $EV_4 > EV_3 > EV_2 > EV_1 > EV_0$. This is attributed to the increase in the extent of crosslinking, which follows the same order (Table 2). It has been found that the tensile strength of the mixes does not show a regular increase with the increase in the extent of crosslinking. The tensile strength is found to be a maximum for EV_2. A possible explanation for this behaviour may be obtained from the nature of the stress–strain curves (Fig. 7).

The stress–strain curves indicate that the deformation of EV_0, EV_1 and EV_2 under an applied load is nearly similar in nature but differs from that of EV_3 and EV_4. The stress–strain behaviour of EV_0, EV_1 and EV_2 shows relatively low modulus values at lower strains. But at higher strains ($\geqslant$600%) there is considerable increase in modulus and this may be attributed to strain-induced crystallisation of the polyethylene segments present in the polymer chain. It has already been reported that EVA has a tendency to undergo strain-induced crystallisation at higher strains.[27] The stress–strain curves for EV_3 and EV_4 are similar in nature and can be compared to those of gum vulcanizates of non-crystallisable rubbers. The absence of crystallisation tendency in EV_3 and EV_4 is attributed to their lower elongation resulting from the high extent of crosslinking. This accounts for the lower tensile strength compared with EV_2. Moreover, the tensile properties of EV_4 and EV_3 indicate that further increase in the

Table 4. Mechanical properties of the mixes

Mix number	Modulus at 300% elongation (MPa)	Tensile strength (MPa)	Elongation at break (%)	Tear strength (kN/m)
EV_0	0·50	3·00	1 500	13·6
EV_1	1·50	3·80	1 050	26·6
EV_2	2·00	4·80	875	28·6
EV_3	2·50	3·90	560	31·2
EV_4	2·60	3·91	550	35·1

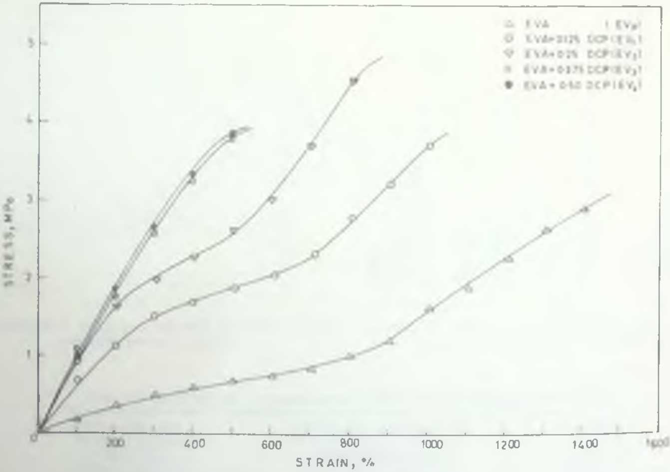

Fig. 7 Stress–strain curves for the mixes.

extent of dynamic crosslinking may have only little influence in improving the properties.

3.3 *Fractographs*

3.3.1 Tensile failure. The tensile fracture surfaces of EV_0 and EV_4 (Figs 8 and 9) reveal that these materials vary in their deformation characteristics under an applied load. The tensile fracture surface of EV_0 (Fig. 8) shows continuous broad cracks with a very smooth surface. This clearly indicates a low tensile strength for the material. On the other hand, the fracture surface of EV_4 (Fig. 9) shows elastic deformation with discontinuous fracture paths and vacuoles all over the surface. Moreover, the fracture surface is found to be extremely rough. These observations may be associated with the high strength of the crosslinked material towards the applied tensile force. The stress–strain curves also support the above views.

3.3.2 Tear failure. The resistance to tearing of elastomers depends on the processes by which stress dissipation near the tip of the growing crack takes place. Several processes, such as slippage or breakage of crosslinks or chain entanglements or the arresting of the growing crack by filler particles, take place during the tear failure of elastomers.[28] The process of stress dissipation can be explored by careful examination of the tear fracture surfaces. The fracture surface of EV_0 (Fig. 10) shows a continuous steady tear path with a smooth surface. Features such as tear branching, folding and striations exhibited by high strength materials are completely absent. This indicates a poor tear resistance for the material. The fracture surface of EV_4 (Fig. 11) shows well-defined vertical striations in the fracture path, like a folded curtain. These vertical striations indicate the resistance offered by the material to the smooth propagation of the tear.[29] As a result, high energy is expended in crack

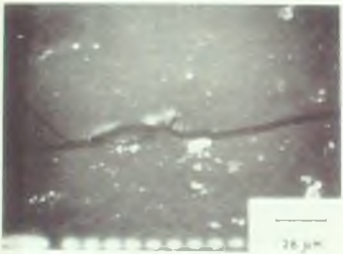

Fig. 8 Tensile failure surface of EV_0 showing continuous smooth cracks.

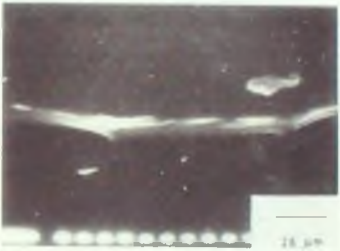

Fig. 10 Tear failure surface of EV_0 showing steady tear path.

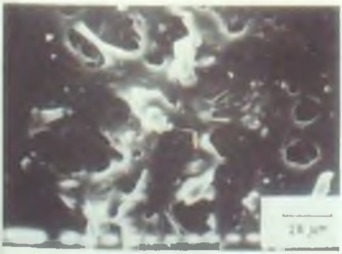

Fig. 9 Tensile failure surface of EV_4 showing elastic deformation and rough zones.

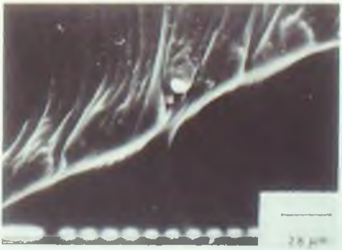

Fig. 11 Tear failure surface of EV_4 showing well-defined vertical striations with a central tear path.

propagation. Measurements of tear resitance also indicated a higher tear strength for EV_4.

4 Conclusions

The following conclusions can be drawn from the present work:

(1) The rheological properties of dynamically crosslinked EVA show that these materials can be processed like thermoplastics by extrusion and injection moulding techniques, since the viscosity at higher shear rate is low.

(2) Dynamic crosslinking increases only slightly the viscosity of the system at high shear rates, but gives reduced swell and improved physical properties.

(3) The shear viscosity values of dynamically crosslinked mixes can be easily found from the empirical equations at the desired shear rate and extent of crosslinking.

(4) Tensile and rheological properties indicate that increasing the extent of dynamic crosslinking beyond 0·5 of DCP has only a slight influence on the properties.

(5) Observations on the fracture surfaces of both crosslinked and uncrosslinked materials show that the patterns developed on the fracture surfaces correlate with their strength and the type of failure.

References

1. WALKER, B. M. *Handbook of thermoplastic elastomers*, Van Nostrand Reinhold Company, New York, 1979.
2. WHELAN, A. and LEE, K. S. (eds) *Developments in rubber technology – 3, Thermoplastic rubbers*, Elsevier Applied Science Publishers Ltd, London, 1982.
3. THORN, A. D. *Thermoplastic elastomers, a review of current information*, Rubber and Plastics Research Association of Great Britain, Shawbury, England, 1980
4. BRYDSON, J. A. In: *Developments in rubber technology – 3, Thermoplastic rubbers*, Whelan, A. and Lee, K. S. (eds), Elsevier Applied Science Publishers Ltd, London, 1982, pp. 1–20.
5. GILBY, G. W. In. *Developments in rubber technology – 3, Thermoplastic rubbers*, Whelan, A. and Lee, K. S. (eds), Elsevier Applied Science Publishers Ltd, London, 1982, pp. 101–44.
6. CAMPBELL, D. S., ELLIOTT, D. J. and WHEELANS, M. A. Thermoplastic natural rubber blends, *NR Technol.*, 9 (1978), p. 21.
7. CORAN, A. Y. and PATEL, R. P. Rubber-thermoplastic composition: Part I, EPDM – Polypropylene thermoplastic vulcanizates, *Rubb. Chem. Technol.*, 53 (1980), p. 141.
8. CORAN, A. Y. and PATEL, R. P. Rubber–thermoplastic composition: Part II, NBR – Nylon thermoplastic elastomeric compositions, *Rubb. Chem. Technol.*, 53 (1980), p. 781.
9. RAMOS-DeVALLE, L. F. and RAMIREZ, R. R. Thermoplastic–guayule rubber blends, composition and mechanical properties, *Rubb. Chem. Technol.*, 55 (1982), p. 1328.
10. FISCHER, W. K. Dynamically partially cured thermoplastic blend of monoolefin copolymer rubber and polyolefin plastic, US Patent 3806558, 1974.
11. AKHTAR, S., DE, P. P. and DE, S. K. Effect of blend ratio, dynamic crosslinking and HAF black on failure properties and hot air and acid ageing resistance of thermoplastic elastomers from natural rubber–high density polyethylene blends, *Mater. Chem. Phys.*, 12 (1985), p. 235.
12. KHANNA, S. K and CONGDON, W. I. Engineering and moulding properties poly(vinyl chloride), acrylonitrile–butadiene–styrene and polyester blends, *Polym. Engg. Sci.*, 23 (1983), p. 627.
13. FOLT, V. L. and SMITH, R. W. Rheology of elastomer blends, *Rubb. Chem. Technol.*, 46 (1973), p. 1193
14. DANESI, S. and PORTER, R. W. Blends of isotactic polypropylene and ethylene–propylene rubbers: rheology, morphology and mechanics, *Polymer*, 19 (1978), p. 448.
15. NAKAJIMA, W. and COLLINS, E. A. Flow-behaviour of elastomers containing crosslinked particles *J. Rheol.*, 22 (1978), p. 547.
16. MONTES, S. A. and PONCE-VELEZ, M. A. Effects of gel and non-rubber constituents on the extrusion properties of guayule rubber, *Rubb. Chem. Technol.*, 56 (1983), p. 1.
17. POWELL, P. C. *Polymer rheology and plastics processing*, The Plastics and Rubber Institute, London 1975, p. 189
18. MENDELSON, R. A. and FINGER, F. L. High density polyethylene melt elasticity – Some anomalous observations on the effects of molecular structure. *J. Appl. Polym. Sci.*, 19 (1975), p. 1061.
19. NEWMAN, S. and TREMENTOZZI, Q. A. Barus effect in filled polymer melts, *J. Appl. Polym. Sci.*, 9 (1965), p. 3071.
20. OVERDIEP, W. S. and VAN KREVELEN, D. W. Studies of Newtonian flow I. Criterion of flow instability, *J. Appl. Polym. Sci.*, 9 (1965), p. 2779.
21. COGSWELL, F. N. Stretching flow instabilities at the exits of extrusion dies, *J. Non-New Fluid Mech.*, 2 (1977), p. 37.
22. KURIAKOSE, B. and DE, S. K. Studies on the melt flow behaviour of thermoplastic elastomers from polypropylene natural rubber blend, *Polym. Engg. Sci.*, 25 (1985), p. 630.
23. KURIAKOSE, B. and DE, S. K. Scanning electron microscopy studies on tensile failure of thermoplastic elastomers from natural rubber-poly(propylene) blend, *Mater. Chem. Phys.*, 12 (1985), p. 157.
24. KURIAKOSE, B. and DE, S. K. Tear and wear of silica filled thermoplastic–natural rubber blend, *Int. J. Poly. Mater.*, in press.
25. *Handbook of Instron UTM 1195*, manual No. M10-4-1(c), Instron Limited, Buckinghamshire, England. Part 2, Section 9, p. 11.
26. ELLIS, B. and WELDING, G. N. *Techniques of polymer science*, Society of Chemical Industry, London, 1964, p. 46.
27. *Encyclopedia of polymer science and technology*, Vol 6, Inter Science Publishers, New York, 1967, p. 399.
28. MATHEW, N. M. and DE, S. K. Scanning electron microscopy studies on tear fracture of natural rubber, *Polymer*, 23 (1982), p. 632.
29. THOMAS, S., KURIAKOSE, B., GUPTA, B. R. and DE, S. K. Scanning electron microscopy studies on tensile, tear and abrasion failure of plasticized poly(vinyl chloride) and copolyester thermoplastic elastomers, *J. Mat. Sci.*, in press.